Progress In Electromagnetics Research, Vol. 137, 453–473, 2013

THE INFLUENCE OF HUMAN HEAD MODEL WEARING METAL-FRAME SPECTACLES TO THE CHANGES OF SAR AND ANTENNA GAIN: SIMULATION OF FRONTAL FACE EXPOSURE

Mohd H. Mat[1, *], Fareq Malek[1], William G. Whittow[2], Suzanna H. Ronald[1], Muhammad S. Zulkefli[1], Norshafinash Saudin[1], and Latifah Mohamed[1]

[1]School of Electrical Systems Engineering, Universiti Malaysia Perlis (UniMAP), Kuala Perlis, Perlis 02000, Malaysia

[2]School of Electronic, Electrical and Systems Engineering, Loughborough University, LEICS LE11 3TU, UK

Abstract—The relationship between specific absorption rate (SAR) and antenna gain inside the head due to the metal-frame spectacles was investigated. The radio frequency (RF) energy source considered is the smartphone used in the frontal face. A computer simulation using CST Microwave Studio 2012 was used for the investigation. Two sets of dipole antennas operated at 900 MHz and 1800 MHz for GSM applications, were used as representative radiation sources from a mobile phone. Parametric studies were conducted to determine the optimum length of the metal rod, and the length was used to study the possibility of RF irradiation of the metal spectacles model. Then, the spectacles model was used as an analysis tool to study the interaction between gain and SAR in the head. The radiation pattern was plotted to identify the causes of the interactions. The gain decreased when the energy source was very close to the spectacles and SAR increased enormously.

1. INTRODUCTION

Through the past few years, mobile communication devices operating in the radio frequency (RF) range have spread into the market very rapidly. This leads to users being exposed to the RF electromagnetic radiation emitted by mobile communication equipment, such as cellular

Received 30 January 2013, Accepted 25 February 2013, Scheduled 28 February 2013

* Corresponding author: Mohd Hafizuddin Mat (hafizuddin.mat@gmail.com).

phones. Concern about possible health effects due to exposures to electromagnetic fields (EMs) has increased among the public and professionals since these communication devices have proliferated around the globe [1–8]. This concern has caused an increase in the research emphasis on analyzing the rate at which electromagnetic radiation is being absorbed by the human body [1–7, 9–17].

Specific absorption (SA) is defined as the quotient of the incremental energy (dE) absorbed by an incremental mass (dm) contained in a volume (dV) of a given density (rho). However, SAR is defined as the rate of energy (dE) absorbed or dissipated in an incremental mass (dm) contained in an incremental volume (dV) of a given density (rho) [1–7, 9–11, 18–41]. Mathematically, SAR can be expressed in watt per kilogram (W/kg) as

$$SAR = \frac{d}{dt}\left(\frac{dE}{dm}\right) = \frac{d}{dt}\left(\frac{dE}{\rho dV}\right) \tag{1}$$

Cooper's initial research [1] considered the implantation of metal inside the head and found that the rate of RF energy absorption was improved in the area. Metal objects, such as spectacles, have received limited attention in the literature; however, several studies have been conducted to investigate the maximum SAR for various shapes of spectacles [2, 11] and glass lens [2, 5]. The paper showed that metallic spectacles can re-distribute the energy produced by the cell phone's antenna, causing the efficiency to drop and the peak SAR to increase. The head also was irradiated from in front of the eye when using realistic, mobile-phone models in [7] to decrease the value of SAR. But there are still uncertainties in study regarding the performance of the antenna and SAR to the human head [15]. The magnetic resonance imaging (MRI) model with the heating effect [26–29, 37, 42–44] was investigated, and it was found that tissue was heated in the presence of implanted medical leads [29]. These papers showed that metal objects close to biological matter may increase SAR in the biological matter.

In the present work, the maximum value of the SAR was investigated intensely by determining the relationship between the maximum absorption rate and the changes in the gain of the antenna. By changing the distance between the antenna and the metal-frame spectacles or head model and observing the results, it was hypothesized that the antenna gain would decrease if the antenna were too close to the metal object and tissue; this could lead to increases in the value of SAR.

2. METHODOLOGY

2.1. Dipole Antennas as Exposure Sources

The RF energy source to be considered is smartphones, which are used often in the frontal face area instead of close to the ear. A dipole is represented as a frontal radiation source used in each simulation. The changes of SAR that were affected by the RF energy coupled with metal spectacles and the location of the antenna with respect to the human face have received limited attention in the literature.

Two half-wave dipole antennas 900 MHz and 1800 MHz were used as the exposure sources for this study. Figure 1 shows the dimensions of the antennas. The S_{11} performance and farfield radiation patterns at 900 MHz and 1800 MHz, shown in Figure 2 and Figure 3 respectively, together with Table 1 summarize the radiation characteristics of the antennas. Since not all radiation patterns from the mobile phones

Table 1. Summary of the characteristics of the radiation.

Characteristics	900 MHz	1800 MHz
Main lobe magnitude	2.3 dBi	2.3 dBi
Main lobe direction	−90.0 deg	90.0 deg
Angular width (3 dB)	76.9 deg	77.5 deg
Efficiency	99.9%	99.42%

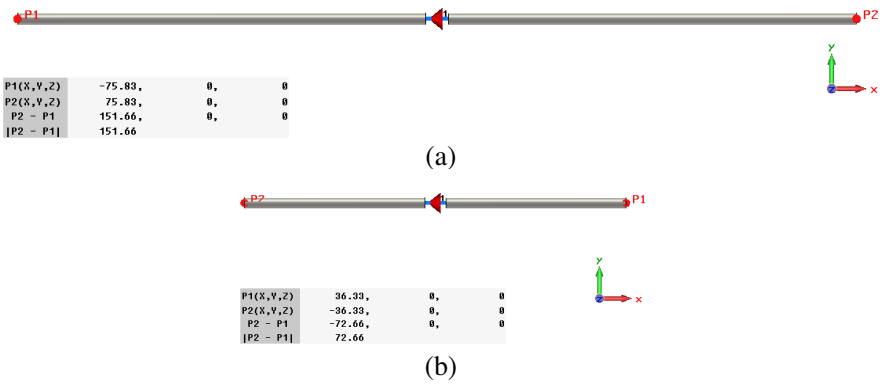

Figure 1. Diagram of dipole antenna with dimensions for (a) 900 MHz and (b) 1800 MHz.

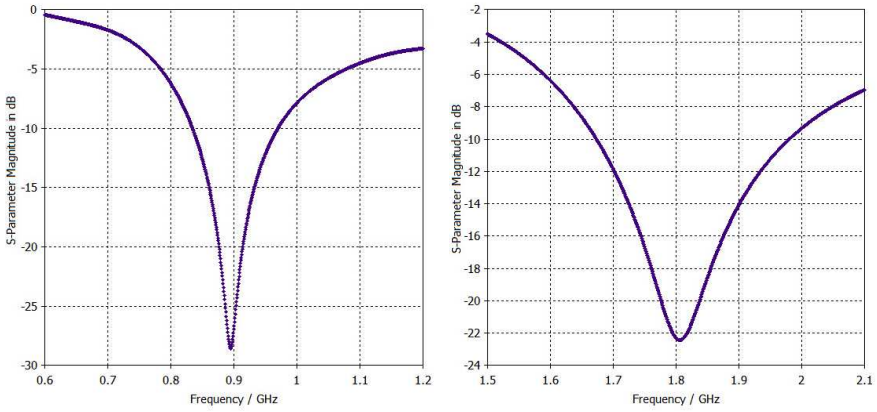

Figure 2. Performance magnitude of dipole antennas S_{11} in dB for (a) 900 MHz and (b) 1800 MHz.

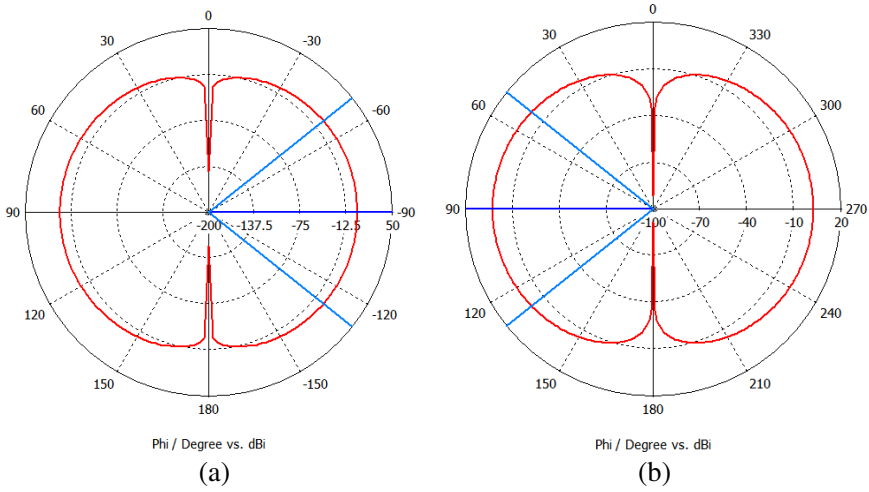

Figure 3. Radiation characteristics of a dipole antenna as a radiation source at 900 MHz: (a) S_{11} magnitude in dB; (b) radiation pattern.

radiated with the same pattern, the radiated field distribution of the dipole antenna was believed to be the most relevant antenna for this work instead of the specific or typical antennas for current mobile phones, which operate in the range of GSM900 and GSM1800 range.

2.2. Head Models

The specific anthropomorphic mannequin (SAM) phantom head model, also called SAM, was provided by CST Microwave Studio (CST MWS) [30], which included the shell and liquid [44–48]. The outer shell of the head had a fixed relative permittivity of 3.5 with an electrical conductivity of 0.0016 S/m in this simulation [6, 47]. Table 2 shows the parameters of the head simulating liquid (HSL) used for both of the GSM frequency ranges used. The results for all simulations were normalized to 1 Watt accepted power, and the worst case scenario was assumed to be the case in which the mobile phone's antenna required more power when operated at a long distance from base stations [31].

This SAM phantom head model was a good choice for observing radiation patterns and for fast calculations, but its accuracy was suboptimal. In the heterogeneous head model, the complex and actual human anatomical structure existed as a voxel data set, which was comparable to the human head, for measuring the absorption of radiation. Thus, the HUGO human head model, also called HUGO, was used to determine the exact location for optimum RF energy absorption inside the human head when a mobile phone was operated in the frontal face area. The advantage of CST Microwave Studio (CST MWS) is that it allows the importation of arbitrary voxel data sets for an accurate SAR study. The most prominent and most often used HUGO model is the anatomical data set of the Visible Human Project. The so-called Voxel Man is based on a dissected male corpse sliced into several thousand layers [26]. The model is performed at the resolution of 1 mm, and different tissue materials were chosen. The area of interest can be selected a priori in a side view and front view. In this study, only the head region was used for the SAR calculation. The frequency-dependent dielectric properties of the tissues used in this model were available in the data sheet of the Federal Communication Commission (FCC) [26, 27]. The HUGO model was used after the SAR validation using SAM phantom head, and, then, the absorption level was compared for the two head models. Illustrations of the SAM and HUGO human head models are shown in Figure 4.

Table 2. Parameters of the head simulating liquid (HSL) [6].

HSL	Permittivity, ε_r	Conductivity (S/m)
900 MHz	41.5	0.97
1800 MHz	40.0	1.40

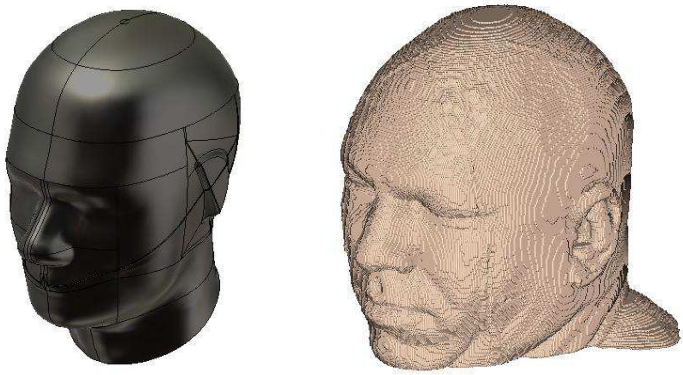

(a) (b)

Figure 4. Two different head models: (a) SAM phantom head and (b) HUGO human body model at a resolution of 1 mm.

2.3. Setups and Results of Metal-frame Spectacles

As mentioned, a scenario was considered in which the incoming radio signal was in a line-of-sight path to a stationary head (frontal face) in free space. Figure 5 illustrates this scenario. Notice that all of the SAR simulations were performed in the frontal face, as would be the case during texting or using various applications.

2.3.1. Phase 1: A Metal Rod as Simple Metal-frame Spectacles

A straight, 2-mm diameter metal rod as simple, metal-frame spectacles and a dipole were aligned horizontally. Two sets of dipole antennas, which were designed earlier for GSM applications and were operated at 900 MHz and 1800 MHz, were used in separate simulations. For the parametric studies, the locations of the dipole antennas with respect to the surface of the SAM were fixed, and only the length of the rod and the distance of its horizontal separation from the SAM were varied. The purpose of this stage was to study the optimum length of the metal rod that would inflict the maximum SAR at both frequencies.

Figure 6 shows the results of parametric studies of the maximum $SAR_{1\,g}$ at 900 MHz and 1800 MHz. The averaging over a 10-g mass of tissue is not shown because the purpose of this in this stage was only to find the optimum length and other parameters. Mass averaging will give approximately the same result. Notice that the maximum SAR without the metal rod was located at the tip of the nose, whereas the maximum SAR was located behind the rod when it was in the frontal

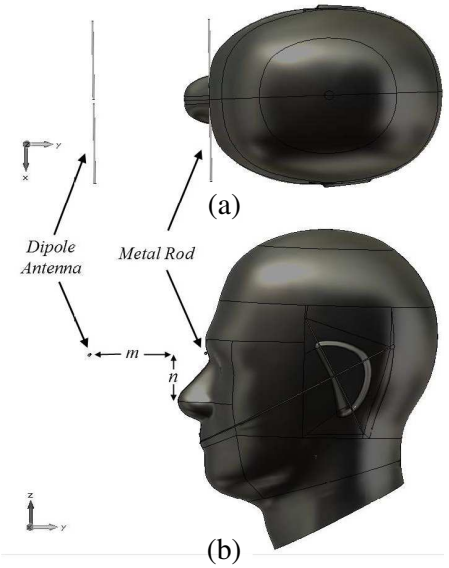

Figure 5. Position of the dipole antenna and metal rod in simulation: (a) top view; (b) side view. The positions are as follows: horizon distances from the dipole to the tip of the nose, $m = 80$ mm, and vertical distances from the tip of the nose to dipole or metal rod, $n = 44$ mm.

Table 3. Relationships between the ranges of optimum length that caused the maximum SAR to the SAM compared to the length of the dipole.

Length	**Frequency (MHz)**	
	900	**1800**
Optimum Metal Rod (mm)	131–160	65–79
Dipole (mm)	151.66	72.66

face. Table 3 summarizes the range of optimum length that resulted in the maximum RF energy absorption by the head.

From Table 3, when the length of dipole within the range of optimum metal rod length, the maximum SAR was found around the eyebrow and the nose. The range separation distance between SAM and the rod for 900 MHz that ranged from approximately 2.5 to 8 mm caused the large SAR. The highest SAR was observed at 7 mm

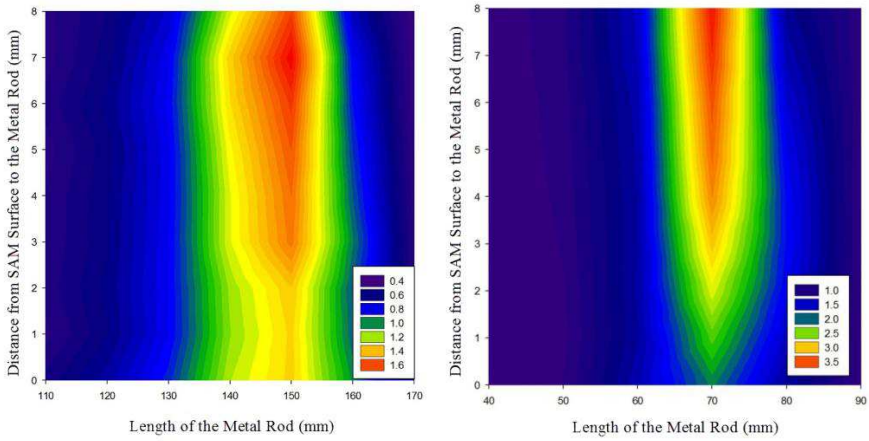

Figure 6. $SAR_{1\,g}$ (W/kg) with increasing length of the metal rod and separation distance from SAM surface at (a) 900 MHz and (b) 1800 MHz.

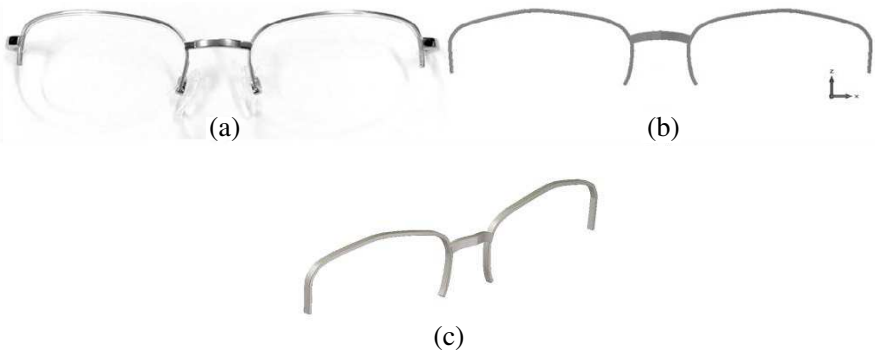

Figure 7. Diagram of front view half rim metal spectacles: (a) actual and (b) after being modeled in the simulation; (c) perspective view of the model.

with a rod length of 150 mm. However, for 1800 MHz, the maximum SAR observed occurred when the rod length was approximately 70 mm. This observation held for both frequencies. The results of this stage proved that a different metal object could resonate again even if the first resonator was transmitting from a safe separation distance. These results led us to the second stage of the study in which we modeled the actual metal spectacles.

Figure 8. Diagram of SAM phantom head-worn, metal-frame spectacles replaced the metal rod exposed to RF radiation from the dipole antenna in the frontal face.

2.3.2. Phase 2: Model Based on the Frame of the Actual Spectacles

The frame of spectacles was modeled carefully by CST MWS using a grid technique to ensure that its dimensions and shape were similar to the actual values and could be fitted to the head model. The distance from the center of the phantom surface to the center of the spectacles was 25 mm. The illustrations of the metal spectacles for both the model and the actual spectacles are shown in Figure 7. In this section, the model was used to replace the metal rod. The location of SAR then was plotted in SAM to observe how the absorption pattern was affected by the realistic model of the frame. The lens and arms were less important [2].

Figures 9(c) and (d) show the SAR averaging over a mass of 1 gram and 10 grams for 900 MHz. The results obtained from the simulated, realistic, metal-frame spectacles showed that a large amount of RF energy was absorbed focally from the top of the eyebrow area to the eyelid region. This possibly caused the absorption of RF energy by the eye. In Figure 9(d), the same effect was found for 10-gram mass averaging.

For both instances of mass averaging, using the 1800-MHz radiation source gave almost no absorption by the eye, but most of the radiation was absorbed by the nose as shown in Figure 10. The SAR values were lower than when the 900-MHz source was used. Thus, the results indicated that the metal object resonated within its specific length range. Within these ranges, the maximum SAR might be obtained. The ranges are shown in Table 3.

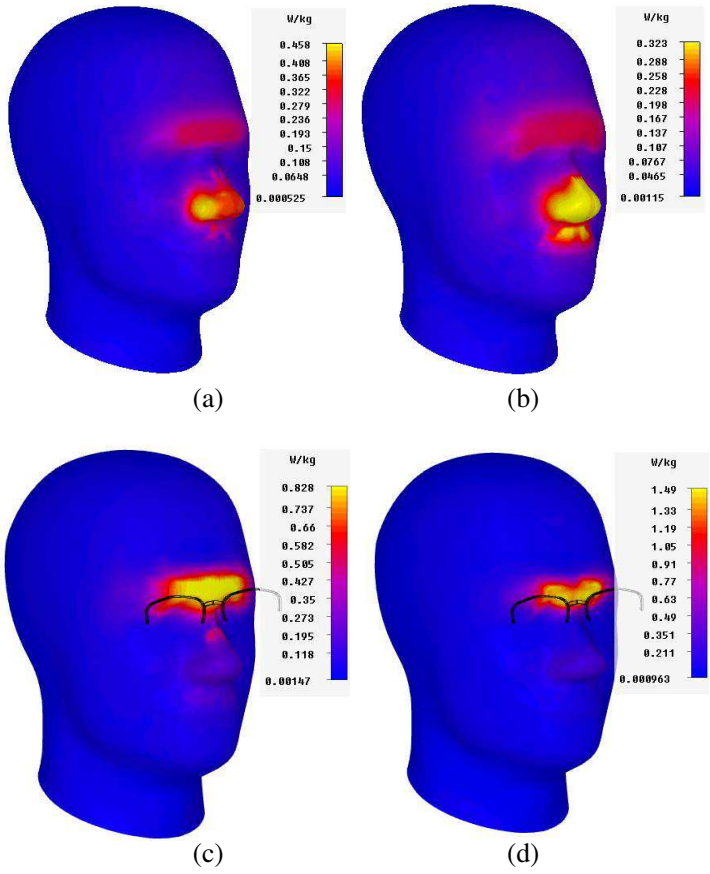

Figure 9. Simulation results at 900 MHz of SAM head without the spectacles for (a) $SAR_{1\,g}$ and (b) $SAR_{10\,g}$ and SAM head worn the spectacles for (c) $SAR_{1\,g}$ and (d) $SAR_{10\,g}$.

2.3.3. Simulation on Realistic Human Head Simulation (HUGO) at 900 MHz

Figure 11 shows the cross-sectional view of HUGO human head simulated over 1 gram mass and 10 gram mass. Each tissue has its own electrical parameter, as discussed in Section 2.2.

For this stage, only a frequency of 900 MHz was used as the radiation source. The frequency of 1800 MHz was not used because the length of the spectacles' frame was far beyond the optimal length, as discussed earlier in Section 2.3.1. The SAR values expected could be much higher if the spectacles' length were reduced within the range

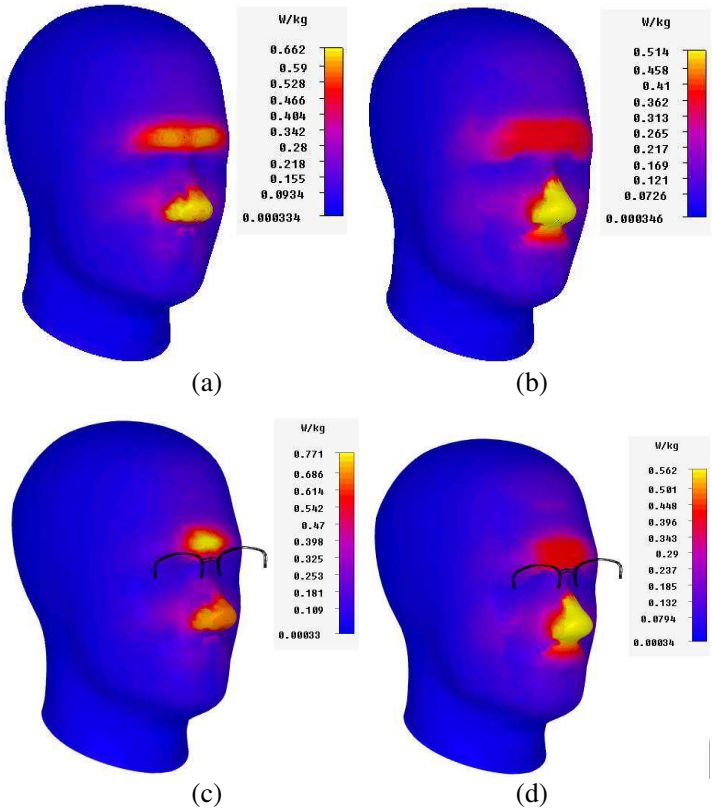

Figure 10. Simulation results at 1800 MHz of SAM head without the spectacles for (a) $SAR_{1\,g}$ and (b) $SAR_{10\,g}$ and SAM head worn the spectacles for (c) $SAR_{1\,g}$ and (d) $SAR_{10\,g}$.

of 65 to 75 mm. However, in the current situation, it is not possible for the spectacles' frame size because we must be able to fit the frame to the head model.

Figures 12(a) and (b) show the vertical cross-sectional view. The cross-section is focused on the eye region to observe the possibility of absorption by the eye. As can be seen the HUGO eye is covered by the eyelid, but, from the results here there is still some RF energy that was able to penetrate into the eye and brain. The averaging of 10 g of mass was used in this simulation due to the same location of the absorption for both averaging as in Figure 11.

In Figure 11, the maximum SAR was plotted only when it was close to the spectacles' frame. In order to observe how deep

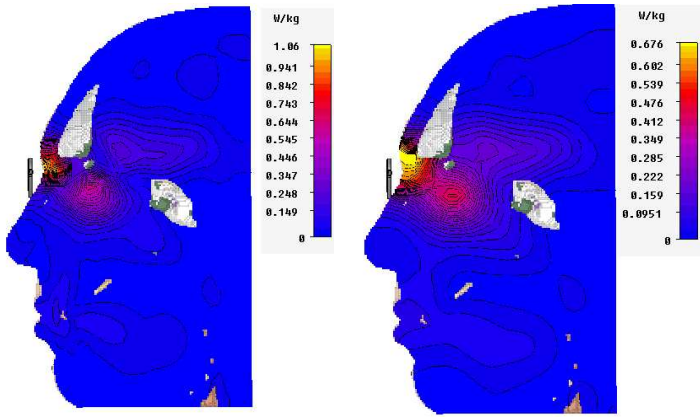

(a) (b)

Figure 11. Cross-sectional view of contour plot for (a) 1 g and (b) 10 g SAR patterns inside HUGO head.

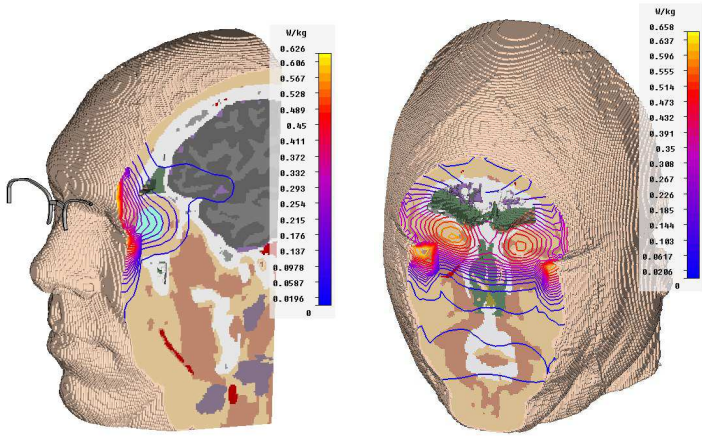

(a) (b)

Figure 12. Cross-sectional view of HUGO head in eye area exposed to the 900 MHz source.

the penetration was, the HUGO was cut into horizontally from the forehead to the nose. Figure 13 summarizes the penetration in six horizontal cross-sections of the HUGO.

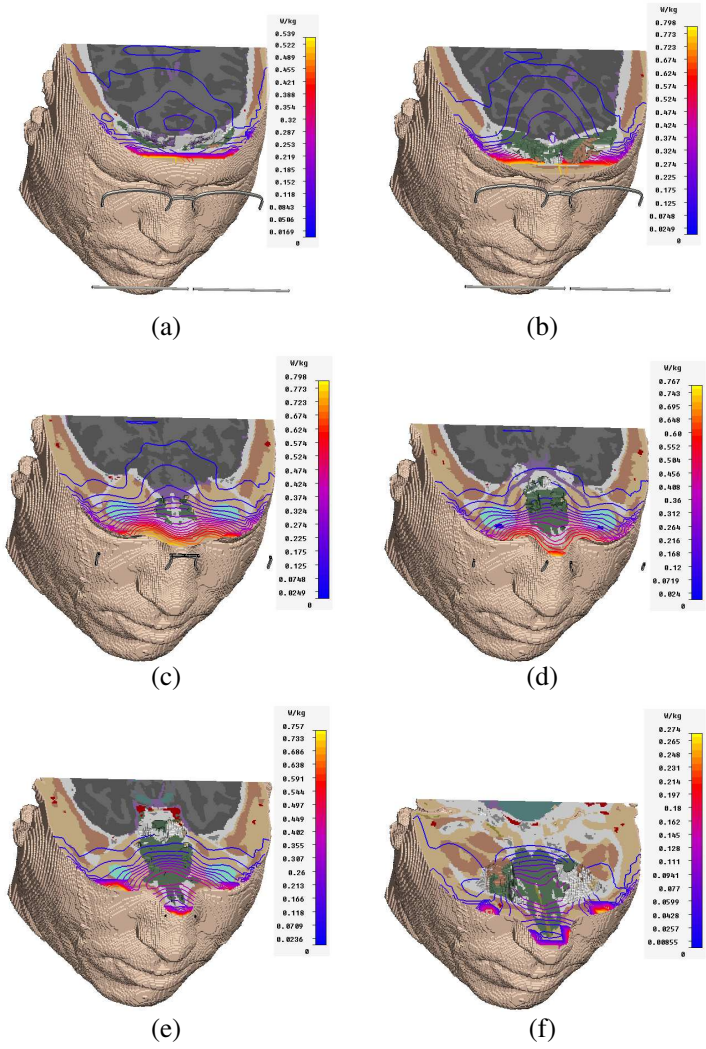

Figure 13. Six horizontal cross sections of the HUGO in six to observe $SAR_{10\,g}$ in the eye.

3. ANTENNA GAINS AND SAR LEVELS AT 900 MHz

For this parametric study, the SAM head was used to decrease the duration of the simulation. Moreover, the SAM was geometrically symmetrical from left to right. Unlike HUGO, the whole body was asymmetrical for the left and right parts. The distance of the antenna

from the metal-frame spectacles varied with the fixed spectacle frame located at 25 mm from the surface of the SAM. Notice here that all models and other electrical conductivity parameters are the same as they were in the previous simulation in order to allow a comparison of the results.

Figure 14 shows the changes of the gain (dipole antenna) for three different situations, i.e., 1) spectacle frame exposed by dipole (spectacle only), 2) SAM phantom head exposed by dipole (head only), and 3) SAM phantom head worn spectacles' frame exposed by dipole.

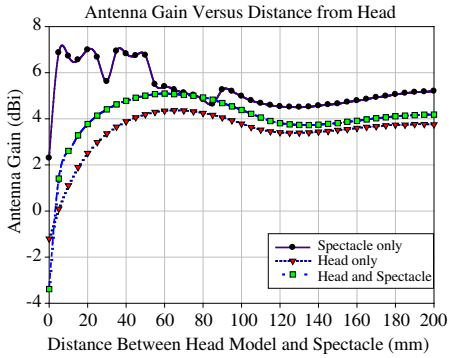

Figure 14. Results of antenna gain for three different situations of exposure at 900 MHz with varied distance between dipole and spectacles' frame.

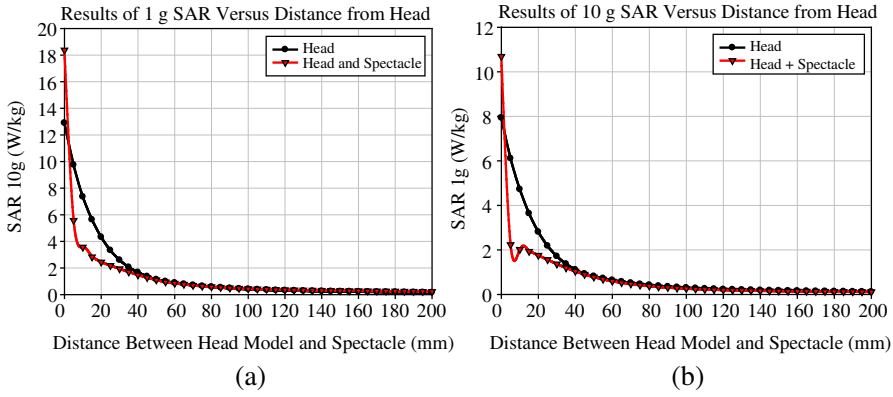

Figure 15. Result of the SAR averaged over (a) 1 g and (b) 10 g mass tissue with increasing distance between the head model and the spectacles (mm).

Only the 900-MHz dipole was used for this analysis, as discussed in the previous section. From the results, both head only and head and spectacle decreased to negative gains for distances from 0–5 mm.

The highest gain was obtained when the SAM was removed. From the plot, the maximum gain of more than 6 dBi was obtained between 5 and 55 mm. From Table 1, it was known that the gain of the initial dipole before any RF interactions occurred was 2.3 dBi. However, in the presence of the SAM, the maximum gain of the antenna gain was changed.

Figures 15(a) and (b) show the SAR averaged over tissue mass with increasing distance between the spectacles' frame and the antenna

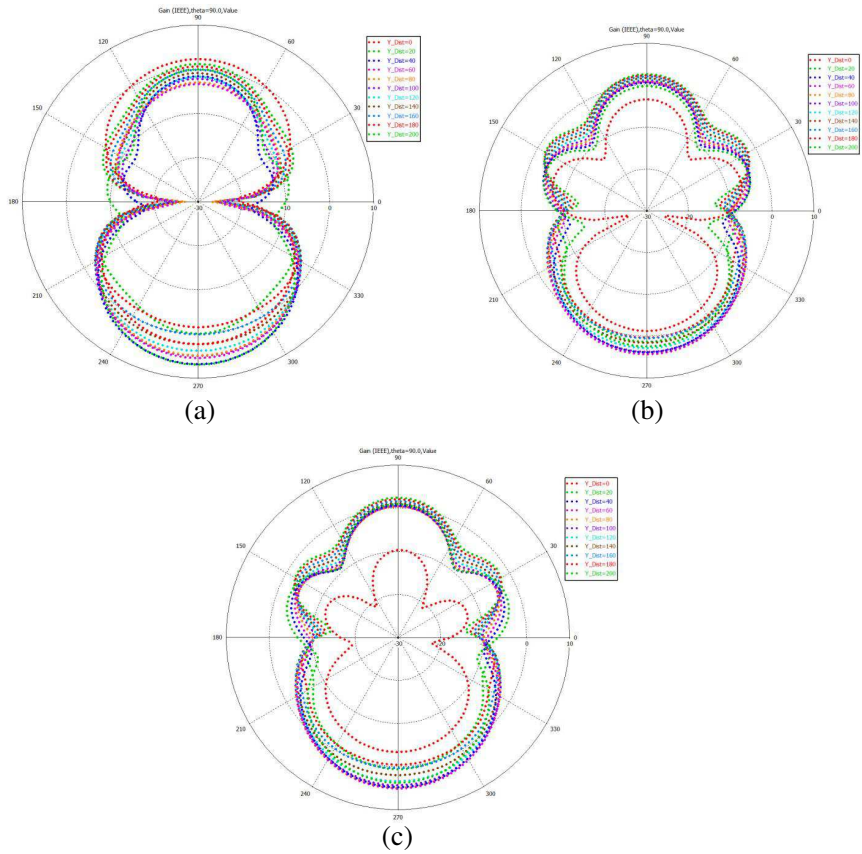

Figure 16. Theta cut at 90 degrees of 900 MHz radiation patterns for three different situations: (a) spectacles only; (b) head only; and (c) spectacles on head.

for 1 gram and 10 grams, respectively. Location of the metal-frame (spectacles) was still at 25 mm from the surface of the SAM. The comparison of the magnitudes of SAR with and without wearing the metal-frame spectacles shows that, by placing the radiation source really close (< 10 mm) to the spectacles' frame, the maximum magnitude (> 1.6 W/kg) was produced inside the SAM head for 1 gram averaging. The same situation was observed from the results of 10 gram SAR. The SAR values for both 1 g and 10 g were reduced significantly at 10 mm and greater (distance between dipole and the spectacles) even by the wearing metal-frame spectacles.

To verify the changes of antenna gain, radiation pattern (polar plot) with theta cut at 90 degrees was performed for three different situations by increasing the distance between the antenna and the spectacles. Compared to the radiation pattern without exposure to anything, as in Figure 3, the exposed radiation pattern showed significant changes in the pattern. The head with and without spectacles showed slight changes of magnitude and main lobe compared to results for the head removed. Figure 16 shows the polar plot. This could explain the basis of SAR changes with variations in the antenna gain.

4. CONCLUSIONS

In this study, the simulations were performed with dipole antennas and it is not directly to extrapolate from the dipole study to a real phone situation, where the return loss, radiation pattern, gain and efficiency is different and the results can be also very different to results obtained in this study. The simulations were performed by varying many parameters that might possibly inflict increased energy absorption from a radiating source to the frontal part of the human head. The simulations were conducted using a symmetrical phantom head and actual tissues base head model. The results confirmed that significant increases of the SAR occurred in the region of the eyes and in certain parts of the head if the user wore metal-frame spectacles when actively using the communication device in frontal head or face areas at 900 MHz. However, at the 1800 MHz range, small spectacles worn by children might increase the absorption to their head by the same phenomenon.

As long the metal-frame spectacles are beyond the resonant frequency range, the absorption rate will be not significant. Furthermore, from the analysis of antenna gain, the absorption of RF energy increased enormously only if the spectacles were really close to the antenna, i.e., 5-mm spacing between the antenna and dipole. As far

as we understood, by holding the communication device far from the head, the rate of energy absorption could be decreased, but, for some situations in which a metal object was present, users should consider using the device at a safe distance from their head and face. In the situation in which a user uses a smart phone really close to metal-frame spectacles, perhaps in speaker-phone mode, the SAR value might be increased. By studying the optimum absorption of RF energy by the human head, it will be possible to investigate the mechanism that changes the SAR in the head when metal spectacles are added. Even though there is still a lot of disagreement about the danger level of SAR, precautions should consider when designing and using an antenna for mobile communications.

REFERENCES

1. Cooper, J. and V. Hombach, "Increase in specific absorption rate in humans from implantations," *Electron. Lett.*, Vol. 32, No. 24, 1996.
2. Whittow, W. G. and R. M. Edwards, "A study of changes to specific absorption rates in the human eye close to perfectly conducting spectacles within the radio frequency range 1.5 to 3.0 GHz," *IEEE Trans. Antennas and Propagation*, Vol. 52, No. 12, 3207–3212, Dec. 2004.
3. Stergiou, K., C. Panagamuwa, W. Whittow, and R. Edwards, "Effects of metallic semi-rimmed spectacles on SAR in the head from a 900 MHz frontal dipole source," *2009 Loughborough Antennas and Propagation Conference (LAPC)*, 721–724, Nov. 16–17, 2009.
4. Whittow, W. G., R. M. Edwards, C. J. Panagamuwa, and J. C. Vardaxoglou, "Effect of tongue jewelery and orthodontist metallic braces on the SAR due to mobile phones in different anatomical human head models including children," *2008 Loughborough Antennas and Propagation Conference (LAPC)*, 293–296, Mar. 17–18, 2008.
5. Bernardi, P., M. Cavagnaro, S. Pisa, and E. Piuzzi, "SAR distribution and temperature increase in an anatomical model of the human eye exposed to the field radiated by the user antenna in a wireless LAN," *IEEE Trans. Microwave Theory Tech.*, Vol. 46, No. 12, 2074–2082, Dec. 1998.
6. Mat, M. H., M. F. B. A. Malek, S. I. Syed Hassan, M. S. Zulkefli, and S. H. Ronald, "Correlation analysis on the specific absorption rate (SAR) between metallic spectacle and pins exposed from

radiation sources," *PIERS Proceedings*, Kuala Lumpur, Malaysia, Mar. 27–30, 2012.

7. Dimbylow, P. J. and S. M. Mann, "SAR calculations in an anatomically realistic model of the head for mobile communication transceivers at 900-MHz and 1.8-GHz," *Phys. Med. Biol.*, Vol. 39, No. 10, 1537–1553, 1994.
8. López-Furelos, A., M. D. M. Miñana-Maiques, J. M. Leiro-Vidal, J. A. Rodríguez-González, F. J. Ares-Pena, and E. López-Martin, "An experimental multi-frequency system for studying dosimetry and acute effects on cell and nuclear morphology in rat tissues," *Progress In Electromagnetics Research*, Vol. 129, 541–558, 2012.
9. Cooper, J. and V. Hombach, "The specific absorption rate in a spherical head model from dipole with metallic walls nearby," *IEEE Trans. Electromagnet. Compat.*, Vol. 40, No. 4, 377–382, Nov. 1998.
10. Bernardi, P., M. Cavagnaro, and S. Pisa, "Evaluation of the SAR distribution in the human head for cellular phones used in a partially closed environment," *IEEE Trans. Electromagn. Compat.*, Vol. 38, No. 3, 357–366, Aug. 1996.
11. Panagamuwa, C. J., W. G. Whittow, R. M. Edwards, and J. C. Vardaxoglou, "A study of the effects of metallic pins on SAR using a specific anthropomorphic mannequin (SAM) head phantom," *2007 European Conference on Antennas and Propagation (EuCAP)*, 1–6, Nov. 11–16, 2007.
12. Fung, L. C., S. W. Leung, and K. H. Chan, "An investigation of the SAR reduction methods in mobile phone applications," *2002 IEEE International Symposium on EMC*, Vol. 2, 656–660, Aug. 2002.
13. Mahmoud, K. R., M. El-Adawy, S. M. M. Ibrahem, R. Bansal, and S. H. Zainud-Deen, "Investigating the interaction between a human head and a smart handset for 4 g mobile communication systems," *Progress In Electromagnetics Research C*, Vol. 2, 169–188, 2008.
14. Nikita, K. S., M. Cavagnaro, P. Bernardi, N. K. Uzunoglu, S. Pisa, E. Piuzzi, J. N. Sahalos, G. I. Krikelas, J. A. Vaul, P. S. Excell, G. Cerri, S. Chiarandini, R. De Leo, and P. Russo, "A study of uncertainties in modeling antenna performance and power absorption in the head of a cellular phone user," *IEEE Trans. Microwave Theory Tech.*, Vol. 48, No. 12, 2676–2685, Dec. 2000.
15. Jung, M. and B. Lee, "SAR reduction for mobile phones based on analysis of EM absorbing material characteristics," *2003 IEEE International Symposium on Antennas and Propagation*, Vol. 2,

1017–1020, Jun. 2003.

16. Manapati, M. B. and R. S. Kshetrimayum, "SAR reduction in human head from mobile phone radiation using single negative metamaterials," *Journal of Electromagnetic Waves and Applications*, Vol. 23, No. 10, 1385–1395, 2009.
17. Chou, H.-H., H.-T. Hsu, H.-T. Chou, K.-H. Liu, and F.-Y. Kuo, "Reduction of peak SAR in human head for handset applications with resistive sheets (R-CARDS)," *Progress In Electromagnetics Research,* Vol. 94, 281–296, 2009.
18. Zhang, M. and A. Alden, "Calculation of whole-body SAR from a 100 MHz dipole antenna," *Progress In Electromagnetics Research*, Vol. 119, 133–153, 2011.
19. Mohsin, S. A., "Concentration of the specific absorption rate around deep brain stimulation electrodes during MRI," *Progress In Electromagnetics Research*, Vol. 121, 469–484, 2011.
20. Cole, K. S. and R. H. Cole, "Dispersion and absorption in dielectrics: I. Alternating current characteristics," *Journal of Chemical Physics*, 341–351, Apr. 1941.
21. Harrington, R. F., *Field Computation by Moment Methods*, Wiley-Interscience and IEEE Press Series on Electromagnetic Wave Theory, 1993.
22. Sullivan, D. M., *Electromagnetic Simulation Using the FDTD Method*, IEEE Press Series on RF and Microwave Technology, 2000.
23. Lancellotti, V., B. P. de Hon, and A. G. Tijhuis, "Scattering from large 3-D piecewise homogeneous bodies through linear embedding via Green's operators and Arnoldi basis functions," *Progress In Electromagnetics Research*, Vol. 103, 305–322, 2010.
24. Mohsin, S. A., "A simple EM model for determining the scattered magnetic resonance radiofrequency field of an implanted medical device," *Progress In Electromagnetics Research M*, Vol. 14, 1–14, 2010.
25. Amjad, A., R. Kamondetdacha, A. V. Kildishev, S. M. Park, and J. A. Nyenhuis, "Power deposition inside a phantom for testing of MRI heating," *IEEE Trans. Magn.*, Vol. 41, 4185–4187, 2005.
26. Mohsin, S. A., N. M. Sheikh, and U. Saeed, "MRI induced heating of deep brain stimulation leads: Effect of the air-tissue interface," *Progress In Electromagnetics Research*, Vol. 83, 81–91, 2008.
27. CST User Interface for Hugo Human Body Model, [online] available: http://www.cst.com/Content/Applications/Article/HUGO+Human+Body+Model.

28. Data sheet, Federal Communication Commission, [online], www.fcc.gov/fcc-bin/dielec.sh-09/2002.
29. Mohsin, S. A., J. Nyenhuis, and R. Masood, "Interaction of medical implants with the MRI electromagnetic fields," *Progress In Electromagnetics Research C*, Vol. 13, 195–202, 2010.
30. CST Microwave Studio in CST Studio Suite 2011 User's Manual, www.cst.com.
31. Mat, M. H., M. F. Malek., S. H. Ronald, and M. S. Zulkefli, "Effects of the metallic spectacles with braces added on specific absorption rate (SAR) exposed to frontal radiation sources," *2011 Loughborough Antennas and Propagation Conference (LAPC)*, 1–4, Nov. 14–15, 2011.
32. Mat, M. H., M. F. B. A. Malek, A. Omar, M. S. Zulkefli, and S. H. Ronald, "Analysis of the correlation between antenna gain and SAR levels inside the human head model at 900 MHz," *2012 Asia-Pacific Symposium on Electromagnetic Compatibility (APEMC)*, 513–516, May 21–24, 2012.
33. Mat, M. H., F. Malek, S. H. Ronald, and M. S. Zulkefli, "A comparative study of simple geometrical head phantoms on specific absorption rates for simulations and measurements at 900 MHz," *2012 International Conference on Biomedical Engineering (ICoBE)*, 330–334, Feb. 27–28, 2012.
34. Catarinucci, L. and L. Tarricone, "New algorithms for the specific absorption rate numerical evaluation based on spherical averaging volumes," *Progress In Electromagnetics Research B*, Vol. 44, 427–445, 2012.
35. Gangwar, R. K., S. P. Singh, and D. Kumar, "SAR distribution in a bio-medium in close proximity with rectangular dielectric resonator antenna," *Progress In Electromagnetics Research B*, Vol. 31, 157–173, 2011.
36. Ikeuchi, R., K. H. Chan, and A. Hirata, "SAR and radiation characteristics of a dipole antenna above different finite EBG substrates in the presence of a realistic head model in the 3.5 GHz band," *Progress In Electromagnetics Research B*, Vol. 44, 53–70, 2012.
37. Montaser, A. M., K. R. Mahmoud, and H. A. Elmikati, "An interaction study between pifas handset antenna and a human hand-head in personal communications," *Progress In Electromagnetics Research B*, Vol. 37, 21–42, 2012.
38. Andújar, A., J. Anguera, C. Picher, and C. Puente, "Human head interaction over ground plane booster antenna technology: Functional and biological analysis," *Progress In Electromagnetics*

Research B, Vol. 41, 153–185, 2012.

39. Otin, R., "Numerical study of the thermal effects induced by a RFID antenna in vials of blood plasma," *Progress In Electromagnetics Research Letters*, Vol. 22, 129–138, 2011.
40. Faruque, M. R. I., M. T. Islam, and N. Misran, "Design analysis of new metamaterial for EM absorption reduction," *Progress In Electromagnetics Research*, Vol. 124, 119–135, 2012.
41. Yanase, K. and A. Hirata, "Effective resistance of grounded humans for whole-body averaged SAR estimation at resonance frequencies," *Progress In Electromagnetics Research B*, Vol. 35, 15–27, 2011.
42. Wang, J., Z. Zhao, J. Song, X. Zhu, Z.-P. Nie, and Q. H. Liu, "Reconstruction of microwave absorption properties in heterogeneous tissue for microwave-induced thermo-acoustic tomography," *Progress In Electromagnetics Research*, Vol. 130, 225–240, 2012.
43. Mat, M. H., M. F. Abd Malek, M. S. Zulkefli, and H. R. Suzanna, "Preliminary study of electromagnetic energy absorption in the head due to the exposure of radio frequency at 900 MHz," *2012 IEEE Symposium on Computers and Informatics (ISCI)*, 228–231, Mar. 18–20, 2012.
44. AlShehri, S. A., S. Khatun, A. B. Jantan, R. S. A. Raja Abdullah, R. Mahmood, and Z. Awang, "Experimental breast tumor detection using nn-based UWB imaging," *Progress In Electromagnetics Research*, Vol. 111, 447–465, 2011.
45. Otin, R. and H. Gromat, "Specific absorption rate computations with a nodal-based finite element formulation," *Progress In Electromagnetics Research*, Vol. 128, 399–418, 2012.
46. Golestanirad, L., A. P. Izquierdo, S. J. Graham, J. R. Mosig, and C. Pollo, "Effect of realistic modeling of deep brain stimulation on the prediction of volume of activated tissue," *Progress In Electromagnetics Research*, Vol. 126, 1–16, 2012.
47. Islam, M. T., H. Z. Abidin, M. R. I. Faruque, and N. Misran, "Analysis of materials effects on radio frequency electromagnetic fields in human head," *Progress In Electromagnetics Research*, Vol. 128, 121–136, 2012.
48. Ibrani, M., L. Ahma, E. Hamiti, and J. Haxhibeqiri, "Derivation of electromagnetic properties of child biological tissues at radio frequencies," *Progress In Electromagnetics Research Letters*, Vol. 25, 87–100, 2011.